Analysis of Microwave and Optical Devices by Using Quasi-TEM Finite Element Technique

Ismat Zareen[1], M. Shah Alam[2], and Mahbub Amin[3]

[1]Department of Electrical and Electronic Engineering
Ahsanullah University of Science and Technology (AUST), Dhaka 1208, Bangladesh
[2]Department of Electrical and Electronic Engineering
Bangladesh University of Engineering and Technology (BUET), Dhaka 1000, Bangladesh
[3]Transmission Planning, Technology Division, Grameenphone Ltd., Dhaka, Bangladesh
Contact Email: shalam@eee.buet.ac.bd

Abstract—The quasi-TEM finite element analysis of microwave and optical devices has been carried out in this work. The static approach that involves the solution of Laplace's equation can be utilized to characterize many important properties of microstrip lines, microshield lines, and microwave photonic components. In this work, we have incorporated such an analysis to obtain propagation loss in MMIC transmission lines and high-speed electrooptic modulators on $LiNbO_3$ and GaAs. It is shown that microwave losses play an important role on optical bandwidth of these modulators and the estimation of bandwidth depends on accurate calculation of loss. Here, the Perlow's generalized equation has been used to estimate the propagation loss of MMIC lines and very good agreement with the previously published results has been obtained. Very important microwave properties for the design and optimization of MMIC lines and modulators, such as, microwave effective index, characteristic impedance are also calculated by using the capacitance per unit length. These properties have been used in the estimation loss. The dependence of microwave properties with the structural parameters are also investigated and it has been found that considering a dielectric material lossless always lead to an over estimation of optical bandwidth of modulators.

Keywords—MMIC transmission lines, electrooptic modulators, propagation loss, optical bandwidth, finite element analysis.

I. INTRODUCTION

THE accurate analyses of microwave and optical devices have been always a challenge and in the past decade, various analysis methods have been developed and various applications have been shown in the literature. Among the various types of transmission lines, such as arbitrary cross section microstrip lines, V-shaped, W-shaped microshield lines [1]-[5] have been proposed for microwave integrated circuits (MICs) and monolithic microwave integrated circuits (MMICs) by many researchers around the world.

These lines have gathered much interest for microwave propagation as they posses reduced radiation loss and electromagnetic coupling and offer a wide range of characteristic impedance values as compared to conventional microstrip lines [1]-[5]. However, the main challenge was to adopt the theoretical analysis technique suitable for the structure and people have been working hard for this. The same problems are there for photonic devices.

Different methods have been used for modeling the MIC and MMIC devices [6]-[12] and microwave photonic devices [6]-[12]. For electromagnetic based analyses, the conformal mapping method (CMM) is used to model these arbitrary cross section transmission lines with an assumption that the metals are infinitely thin and the ground planes are assumed to be of infinite width [2]. But, from practical fabrication point of view, such assumptions are not possible. The Finite Element Method (FEM) in this regard is superior as it can handle the finiteness of metal thickness as well as the substrate and ground planes and gives sufficiently accurate results if a significant number of elements are used [6]-[7], [11]-[12]. Any arbitrary cross section can also be modeled with triangular elements easily [7]. Furthermore, by adaptive meshing large number of elements can be used near the thin and narrow regions, where the field values are very sensitive because of discontinuities and sharp metal edges. Not only metallic edges, dielectric edge problems are also there and this limits the scope of using many numerical methods to photonic integrated circuit problems. The quasi-static analyses may handle many simplified problems, but cannot handle many sophisticated structures. However, with the advent of powerful PCs and with the blessings of meshing software, this technique is adopted with other techniques to generate many useful characteristics of photonic and microwave devices.

In this work, the FEM has been used for the analysis of such quasi-TEM transmission lines with an emphasis to the analysis of loss. The partial differential equation (PDE) toolbox of MATLAB is used here for preprocessing and solving Laplace's equation using quadratic triangular

elements and adaptive meshing. Microshield lines on isotropic and anisotropic substrates and coplanar waveguides (CPWs) of electrooptic modulators (EOM) are considered as examples in this work. Important microwave properties for the design of MICs and MMICs, such as, microwave effective index, characteristic impedance, and propagation loss are calculated. The propagation loss is calculated using the Perlow's generalized equation [9]. The Perlow's equation uses effective microwave index of the line, operating frequency, the capacitance of the line and the capacitance of air-filled transmission line having the dimension altered by the skin-depth, and gives loss accurately when compared with the published results [11]. The results of this work show excellent agreement with the previously published theoretical and experimental results. Furthermore, optical response and 3-dB bandwidth of modulators have been calculated and the effect of dielectric loss has been demonstrated.

2. QUASI-TEM ANALYSIS

In the quasi-TEM analysis, the two-dimensional Laplace's equation of the following form is usually solved to obtain the potential distribution across the cross section of the structure:

$$\varepsilon_{xj} \frac{\partial^2 \phi_j(x,y)}{\partial x^2} + \varepsilon_{yj} \frac{\partial^2 \phi_j(x,y)}{\partial y^2} = 0 \qquad (1)$$

Here ε_{xj} and ε_{yj} are the relative permittivities in the x and y directions, respectively, of electrically anisotropic substrate of jth region and they are same for isotropic material in the structure. During the discretization process, the electrode region if any will be neglected and Dirichlet type boundary conditions are to be applied on the electrode surface and on the boundary of the structure. By discretizing the cross section with many Lagrange type triangular elements and solving the Laplace's equation (1), the nodal values of the electric potential can be obtained. Once the potential is known, both the horizontal and the vertical component of the electric field can be determined by taking the negative of gradient of the potential.

The capacitance, C, per unit length can be calculated by using the energy expression as

$$C = \frac{2W}{V^2} = \frac{\iint [\varepsilon] |\nabla \phi|^2 \, dxdy}{(\phi_2 - \phi_1)^2}, \qquad (2)$$

where V is the potential difference between the conductors and W is the electrostatic energy. However, the realization of (2) in the FEM is achieved by summing up the contribution from all the elements over the cross section and ϕ_2 and ϕ_1 are the potentials on the electrode and the ground, respectively. Replacing the dielectric materials by free space (air), C_0, the capacitance of air-filled transmission line can be calculated. Then, the microwave effective index, N_m, and

the characteristic impedance, Z_c, of the electrode can be calculated [3], [11]-[12]. The attenuation constant due to the conductor loss can be calculated from the per-unit-length capacitance of the air-filled line using Perlow's generalized equation as [9]

$$\alpha_c = \pi N_m \frac{f}{0.2998} \left[1 - \frac{C_0'}{C_0} \right] \times 8.686 \text{ (dB/m)}, \qquad (3)$$

where f is the operation frequency in GHz, C_0' is the capacitance of the air-filled microwave transmission line having the conductor dimension reduced by the skin-depth. The frequency dependent skin-depth, δ_s, however, can be calculated using

$$\delta_s = \frac{1}{\sqrt{\pi f \mu \sigma}}, \qquad (4)$$

where $\mu = \mu_0 = 4\pi \times 10^{-7}$ H/m for non-magnetic material, and σ is the conductivity of the material. The new reduced dimensions were obtained by taking a reduction of $\delta_s/2$ from each metal surface. The component of the attenuation constant due to losses in the dielectrics can be calculated as [5]

$$\alpha_d = \pi N_m \frac{f}{0.2998} \tan \delta \times 8.686 \text{ (dB/m)}, \qquad (5)$$

if tan-delta ($\tan \delta$), the loss-tangent of the material is known. Though the calculation of the attenuation using (3) and (5) use capacitance of the static analysis and the operation frequency directly, they give good estimations of loss as they incorporate the skin effect in the conductor and the loss-factor of the dielectric material, respectively. However, when the dielectric loss is included, then the total frequency dependent loss may be given by

$$\alpha(f) = \alpha_C \sqrt{f} + \alpha_d f. \qquad (6)$$

If α_c and α_d are normalized at 1 GHz, then f is given in GHz. Here α_c is the conductor loss in decibels per (square root of GHz×cm) and α_c is the total dielectric loss in units of decibels per (GHz×cm). The dielectric loss can arise from different lossy dielectric regions, and in that case losses of different dielectric regions are summed up to obtain the total dielectric loss.

3. SIMULATION RESULTS AND DISCUSSION

3.1 MMIC Transmission Lines

First, let us consider a microshield line, which is widely used in many MMICs. We consider a V-shaped microshield line as shown in Fig. 1. This type of structure offers a wide range of values of their microwave properties and their properties are easily tailorable. The metallization of the substrate boundary is V-shaped and is grounded in this case.

The FEM can easily be used to model this structure, however, the air region above the strip, together with the V-shaped substrate, need to be enclosed by shielding wall to obtain a finite region for the analysis. Fig. 2 shows the potential distribution over the cross section of the line. The potential field is concentrated about the metallic strip conductor. Here $d_1=d_2$, $W=b+d_1+d_2$, $T=1\mu$m,
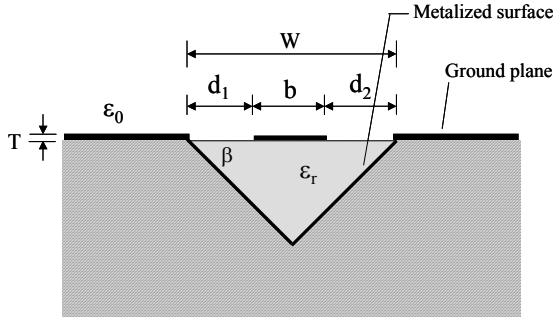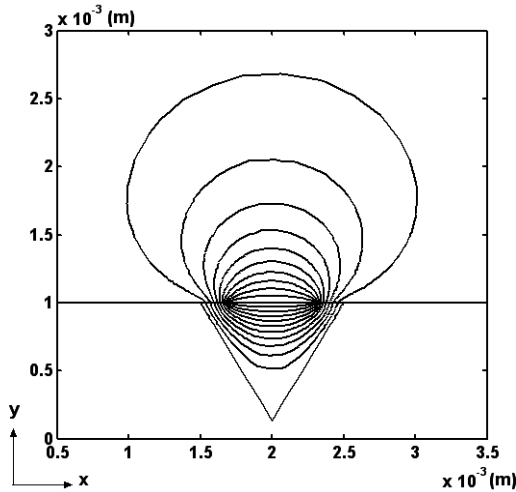

Fig. 1. Cross section of V-shaped micro-shield line.

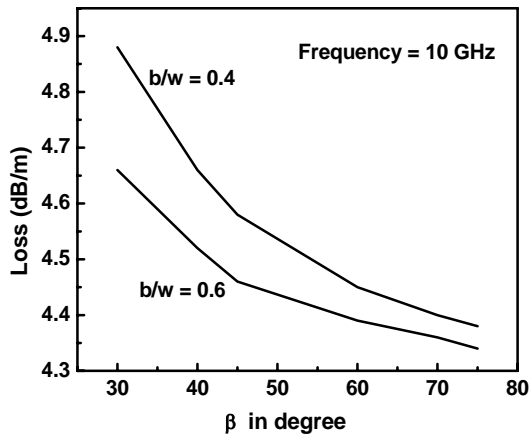Fig. 2. Potential distribution over the cross section of the V-shaped microshield line.

Fig. 3. Propagation loss in the V-shaped microshield line.

$\beta=60°$, and $\varepsilon_r=2.55$. In Fig. 3, we show the propagation loss as a function of β at a frequency of 10 GHz. In this case, the propagation loss includes both the losses due to conductor and dielectric material. The Perlow's equations (3) and (5) are employed in (6) to obtain the total loss coefficient.

It can be seen in Fig. 3 that at lower values of β, the higher is the b/w ratio, and the smaller is the loss in decibels. It can also be seen that for b/w=0.6, the propagation loss does not change for β greater than 45° and for b/w=0.4, the loss decreases with increasing β.

Secondly, we consider a coupled microstrip line, which is another widely used microstrip line in MMICs. Fig. 4 shows a cross section of the coupled microstrip line. In our analysis, the physical dimensions and material constants considered are: l=15mm, h_1=9.0mm, t=0.3mm, h_2=1.0mm, w=3mm, s=10mm, $\sigma=10^5$s/m, ε_r=9.8 and $\tan\delta$=0.0001. During analysis, the potential on the electrodes are ϕ_1=1.5V, while that on the shielding wall is 0V.

In Fig. 5, we show the potential distributions of odd mode and even mode supported by the structure. For odd mode shown in Fig. 5(a), two peaks of opposite signs are seen around the strip conductors, which can be realized by setting equal and opposite voltages on the strips. On the other hand, even modes can be realized by setting equal voltages with same polarity on both the conductors. As can be seen in Fig. 5(b), two peaks of same signs are seen around the strip conductors.

In Fig. 6, we show total loss versus strip width in a coupled microstrip of Fig. 4. The total loss has been calculated for both the odd mode and even mode using the Perlow's equations. The effect of strip thickness has also been shown here. As the strip thickness increases, the propagation loss also increases and the loss is greater for odd mode than the even mode for any thickness of the strip.

3.2 Microwave Photonic Devices

Next, we consider microwave photonic devices and analyze them using the techniques described in the previous section. A coplanar waveguide (CPW) for an electrooptic Machzehnder type modulator is shown in Fig. 7 [13]. Here, a silica buffer layer is there in between the electrodes and the LiNbO$_3$. LiNbO$_3$ is a uniaxial anisotropic material while the silica is a isotropic material. The approach developed here
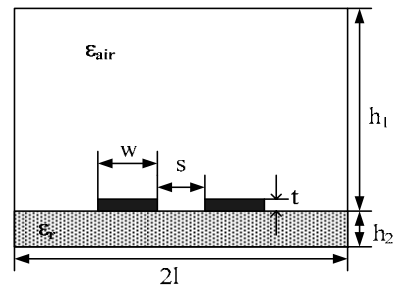

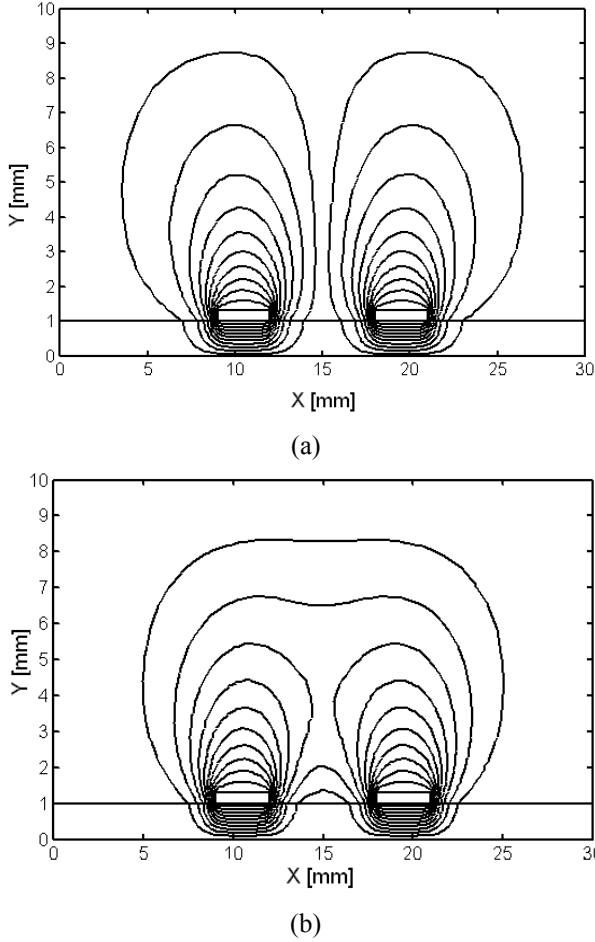Fig. 4. Cross section of coupled microstrip line.

(a)

(b)

Fig. 5. Potential distributions over the cross-section, (a) odd mode, (b) even mode.
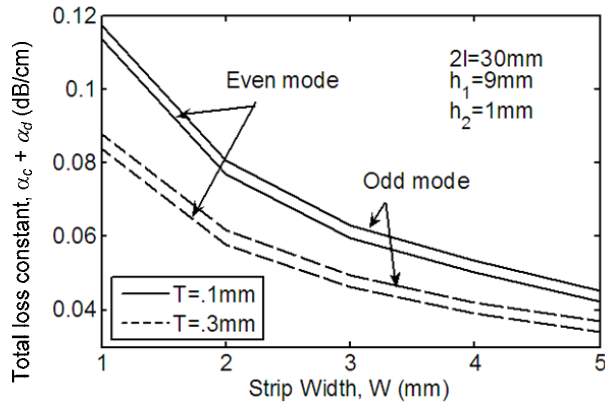

Fig. 6. Total loss versus strip width in coupled microstrip line.

in this work is also applicable in this case. However, in order to obtain the convergence in this case a huge number of elements are required. The relative dielectric constants of LiNbO$_3$ substrate were 28 and 43 in perpendicular and parallel directions to the substrate surface and for silica it was 3.9. In this case, the hot central electrode width S, gap

width G, and buffer layer thickness B, were taken as 8μm, 15μm and 1.2μm, respectively. Fig. 8 shows the contour plot for the potential distribution over the cross section of CPW, where the thickness of T was taken to be 10μm. As expected the figure shows that the potential field surrounds the central hot conductor.

In Fig. 9, the results of loss are compared with those of Rahman and Haxha [13]. The solid lines representing our results agree very well with the results of Rahman and Haxha [13] shown by dark circles for lower values of B. At higher values of B, the results do not agree well. However, in the calculation of capacitance, we took the contribution from all the elements over the cross section and used more than 40000 elements in the discretization process. As can be seen that with the increase in buffer layer thickness loss decreases.

The optical response of a modulator is determined by the microwave propagation characteristics of the electrode, namely, the effective index of the microwave, N_m, the characteristic impedance, Z_C, and the overall propagation losses [7]. The general equation of the optical response is given as [7]-[8]:

$$m(f) = \left| \frac{1 - S_1 S_2}{(1 + S_2)\left[\exp(j2u_+) - S_1 S_2 \exp(-2ju_-)\right]} \right.$$
$$\left. \times \left[\exp(ju_+)\frac{\sin u_+}{u_+} + S_2 \exp(-ju_-)\frac{\sin u_-}{u_-}\right] \right| \tag{7}$$

where

$$u_\pm = \frac{1}{c}\pi f L(N_m \mp N_o) - j\frac{1}{2}\alpha L ,$$

$$S_1 = \frac{Z_1 - Z_C}{Z_1 + Z_C} ,$$

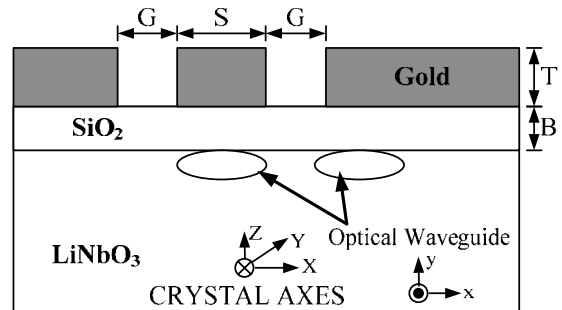$$S_2 = \frac{Z_2 - Z_C}{Z_2 + Z_C} ,$$

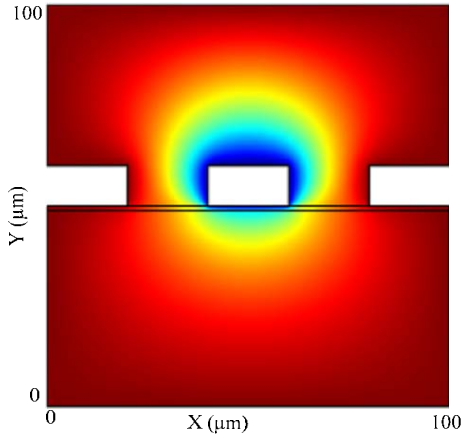Fig. 7. Schematic of Mach-Zehnder EOM.

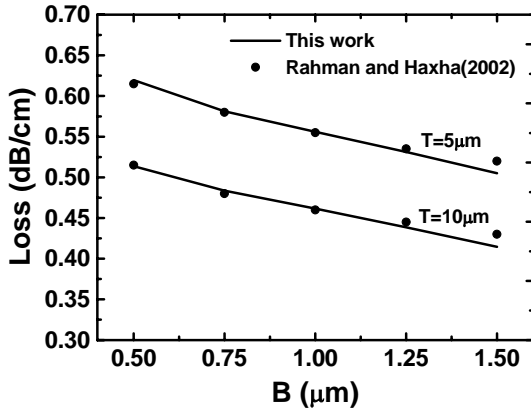Fig. 8. Potential distribution over the cross section of the EOM.

Fig. 9. Loss versus buffer layer thickness.

and Z_C, Z_1, and Z_2 are the microwave characteristic impedance, the microwave generator's internal impedance, and the shunted loaded impedance, respectively. Here N_m, is the microwave effective index, N_o is the optical effective index, α represents overall microwave and dielectric losses, and *c* is the velocity of light [5]. Under the impedance-matching condition, $Z_C = Z_1 = Z_2$, which is often set to 50 Ω, the bandwidth is limited by the velocity mismatch and the total microwave loss, and thus the optical response equation can be reduced to

$$m(f) = \left[\frac{1 - 2e^{-\alpha L}\cos 2u + e^{-2\alpha L}}{(\alpha L)^2 + (2u)^2} \right]^{1/2}, \quad (8)$$

where

$$u = \frac{1}{c}\pi f L (N_m - N_o) \text{ and } \quad \alpha = \alpha_C \sqrt{f}.$$

The bandwidth of an optical modulator primarily depends on the phase mismatching between the optical and

microwave phase velocities. However, when matched, maximum optical bandwidth is achieved and this value is limited by the total microwave loss. The 3-dB modulation bandwidth Δf is usually defined such that $20 \log_{10}\left[m(\Delta f) \right]$ is -3dB, where *m(f)* is the optical response.

Variation of the 3-dB bandwidth with the buffer layer thickness for different metal electrode losses are considered, but the effect of impedance mismatch is neglected. In this case the length of the electrodes, L, is taken as 2.7 cm. When only the conductor loss is considered and the dielectric loss is neglected, bandwidths calculated by using (8) are shown by solid lines in Fig. 10. It can be noted that for T = 20μm, 37.37 GHz maximum bandwidth is reached when N_m=N_o, for B=0.477μm. It can be also noted that for T=15μm, maximum bandwidth is reached when B=0.78 μm.

However, 33.39 GHz maximum value is lower than that for 20 μm, as microwave loss is larger in this case. As the dielectric loss is proportional to the operating frequency, if the dielectric loss is ignored at higher operating frequency the total microwave loss can be significantly underestimated and the estimated bandwidth shows larger value. Variations of the optical bandwidth with the buffer layer thickness B, when the dielectric losses are included, are shown by dashed lines. It can be noted that by neglecting dielectric loss, optical bandwidth could be overestimated by as much as 30%. This error will be even higher when the operating frequency is also higher as the dielectric loss increases faster
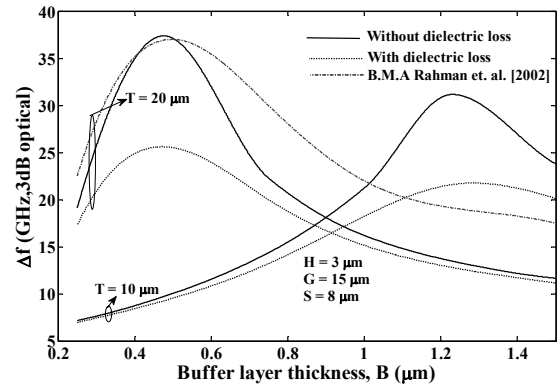

Fig. 10. Variation of the 3-dB optical bandwidth Δf with the buffer layer thickness B for different electrode thickness, T. than the conductor loss with the operating frequency [13].

In the figure, we have also shown the results without dielectric loss calculated by B.M.A Rahman [13] using dashed dotted lines for T = 20 μm. Our results of this case agree with their result [13] for this buffer layers upto the peak value, but larger difference can be seen when buffer thickness is increases. The bandwidth of an optical modulator primarily depends on the phase mismatching between the optical and microwave phase velocities. However, when they are matched, maximum optical

bandwidth is achieved, and this value is limited by the total microwave loss [13]. The 3-dB modulation bandwidth Δf is such that where $20\log_{10}[m(\Delta f)]$ is −3dB. Variation of optical bandwidth with the variation of buffer layer thickness B is analyzed below.

Finally, we considered a GaAs/GaAlAs EOM. Fig. 11 shows the potential distribution, while Fig. 12 shows estimated bandwidth of such a modulator. Variation of the 3-dB optical bandwidth with the buffer layer thickness for different metal electrode losses are considered, but the effect of impedance mismatch is neglected. In this case the length of the electrodes, L is taken as 2cm. When only the conductor loss is considered and the dielectric loss is neglected, bandwidths calculated by using equation (8) are shown by solid lines in Fig. 12. It can be noted that for T = 1μm, 122.8 GHz maximum bandwidth is reached when N_m = N_0 = 2.30 for B = 0.96 μm. It can be also noted that for T = 2μm, maximum bandwidth
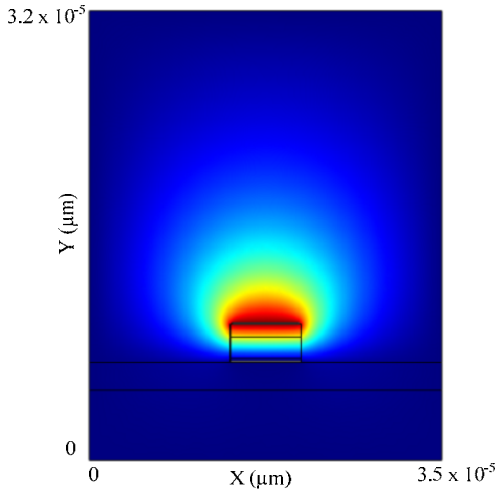

Fig. 11. Potential distribution of GaAs/GaAlAs EO modulator.
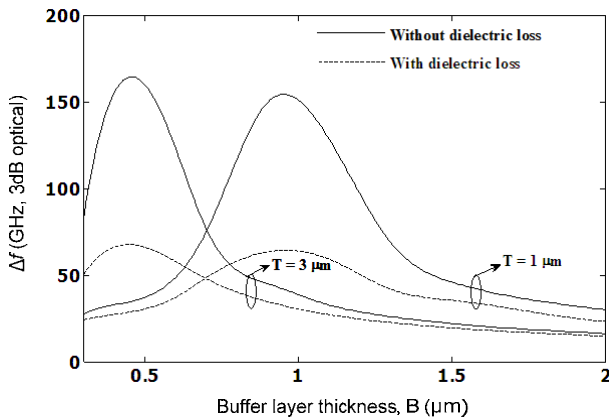

Fig. 12. Optical response for different electrode thickness.

is reached when B equals to 0.64μm. However, this 124.5 GHz maximum value is greater than that for 1μm, as microwave loss is larger in this case.

However, as the dielectric loss is proportional to the operating frequency, if the dielectric loss is ignored at higher operating frequency the total microwave loss is significantly underestimated. Variations of the optical bandwidth with the buffer layer thickness B, when the dielectric losses are included, are shown by dashed lines. It can be noted that by neglecting dielectric loss, optical bandwidth could be overestimated by more than 150%. This error will be even higher when the operating frequency is also higher as the dielectric loss increases faster than the conductor loss with the operating frequency.

4. CONCLUSIONS

An analysis of loss of MIC and MMIC transmission lines on isotropic or anisotropic substrates, and the effect of microwave loss on optical bandwidth of EOM have been shown in this work. With the help of quasi-TEM approximations, microwave properties, such as, microwave effective index, characteristic impedance and propagation loss are calculated by using the capacitance per unit length of the line/guide. The Perlow's generalized equation has been used successfully to evaluate the propagation loss in MMICs and CPWs of Mach-Zehnder type EOM. The results were verified with the previously published results. Thus, using a quasi-TEM finite element analysis, microwave characterization of various inhomogeneous transmission lines or guides are extractable and the dependence of microwave properties and optical response of EOM with the structural parameters, which are essential for the design of MICs, MMICs, and photonic integrated circuits, can be established.

REFERENCES

[1] N. Yuan, C. Ruan, and W. Lin, "Analytical analyses of V, Elliptic, and Circular-Shaped Microshield Transmission Lines," *IEEE Trans. on Microwave Theory and Tech.*, vol. 42, no. 5, pp. 855-858, 1994.

[2] K. M. Cheng and I. D. Robertson, "Simple and Explicit Formulas for the Design and Analysis of Asymmetrical V-Shaped Microshield Line," *IEEE Trans. on Microwave Theory and Tech.*, vol. 43, no. 10, pp. 2501-2504, 1995.

[3] V. Milanovic, M. Gaitan, E. D. Bowen, and M. E. Zaghloul, "Micromachined Coplanar Waveguides in CMOS Technology," *IEEE Microwave and Guided Wave Lett.*, vol. 6, no. 10, pp. 380-382, 1996.

[4] M. Ozgur, V. Milanovic, C. Zincke, M. Gaitan, and M. E. Zaghloul, "Quasi-TEM Characteristic Impedance of Micromachined CMOS Coplanar Waveguides," *IEEE Trans. on Microwave Theory and Tech.*, vol. 48, no. 5, pp. 852-854, 2000.

[5] M. Tanabe, M. Nishitsuji, Y. Anda, and Y. Ota, "A Low-Impedance Coplanar Waveguide Using an SrTiO$_3$ Thin Film

for GaAs Power MMICs," *IEEE Trans. on Microwave Theory and Tech.*, vol. 48, no. 5, pp. 872-874, 2000.

[6] Z. Pantic and R. Mittra, "Quasi-TEM Analysis of Microwave Transmission Lines by the Finite-Element Method," *IEEE Trans. on Microwave Theory and Tech.*, vol. MTT-34, no. 11, pp. 1096-1103, 1986.

[7] M. S. Alam, K. Hirayama, Y. Hayashi, and M. Koshiba, "Analysis of shielded microstrip lines with arbitrary metallization cross section using a vector finite element method," *IEEE Transactions on Microwave Theory and Techniques*, vol. 42, no. 11, pp. 2112—2117, 1994.

[8] M. S. Alam, M. Koshiba, K. Hirayama, and Y. Hayashi, "Hybrid-mode analysis of multilayered and multiconductor transmission lines," *IEEE Transactions on Microwave Theory and Techniques*, vol. 45, no. 2, pp. 205-211, 1997.

[9] L. Zhu and E. Yamashita, "Effects of conductor edge profile on Transmission Properties of Conductor-Backed Coplanar Waveguides," *IEEE Trans. on Microwave Theory and Tech.*, vol. 43, no. 4, pp. 847-853, 1995.

[10] S. M. Perlow, "Analysis of Edge-Coupled Shielded Strip and Slabline Structures," *IEEE Trans. on Microwave Theory and Tech.*, vol. MTT-35, no. 5, pp. 522-529, 1987.

[11] M. E. Goldfarb and A. Platzker, "Losses in GaAs Microstrip," *IEEE Trans. on Microwave Theory and Tech.*, vol. 38, no. 12, pp. 1957-1963, 1990.

[12] Y. Yan and P. Pramanick, "Finite-Element Analysis of Generalized V- and W- Shaped Edge and Broadside-Edge-Coupled Shielded Microstrip Lines on Anisotropic Medium," *IEEE Trans. on Microwave Theory and Tech.*, vol. 49, no. 9, pp. 1649-1957, 2001.

[13] B. M. A. Rahman and S. Haxha, "Optimization of Microwave Properties for Ultrahigh-Speed Etched and Unetched Lithium Niobate Electrooptic Modulators," *Journal of Lightwave Technology*, vol. 20, no. 10, pp. 1856-1863, 2002.

[14] COMSOL Multiphysics, Version 3.2, September 2003.

[15] J. Shin, C. Ozturk, S. R. Sakamoto, Y. J. Chiu, and N. Dagil, "Novel T-Rail Electrodes for Substrate Removed Low-Voltage High-Speed GaAs/AlGaAs Electrooptic Modulators," *IEEE Transaction on Microwave Theory and Techniques*, vol. 53, no. 2, pp. 636-643, 2005.

[16] W. Pascher, J. H. Den. Besten, D. Caprioli, X. Leijtens, M. Smit, and R. Van. Dijk, "Modeling and design of a travelling-wave electro-optic modulator on InP," *Journal of Optical and Quantum Electronics,* vol. 35, Issue 4, pp. 453-456, 2003.

[17] P. Tang, A. L. Meier, and B. W. Wessels, "Low-Loss Electrooptic $BaTiO_3$ Thin Flim Waveguide Modulator," *Optics Letters*, vol. 30, Issue 3, pp. 254-256, 2005.

[18] B. M. A. Rahman, V. Haxha, S. Haxha, and K. T. V. Gratan, "Design Optimization of Polymer Electrooptic Modulators," *Journal of Lightwave Technology*, vol. 24, no. 9, pp. 3506-3513, 2006.

[19] Y. Cui and P. Berini, "Modeling and Design of GaAs Travelling-Wave Electrooptic Modulators Based on the Planar Microstrip Structure," *Journal of Lightwave Technology*, vol. 24, Issue 6, pp. 2368-2379, 2006.

[20] C. Angulo Barrios, V. R. Almeida, R. Panepucci, and M. Lipson, "Electrooptic Modulation of Silicon-on-Insulator Submicrometer-Size Waveguide Devices," *Journal of Lightwave Technology*, vol. 21, Issue 10, pp. 2332-2339, 2003.

[21] Q. Lu, Weihua B. Guo, and J. F. Donegan, "Design of Low VП High-Speed GaAs Travelling-Wave Electrooptic Phase Modulators Using an n-i-p-n Structure," *Journal of Photonics Technology Letters*, vol. 20, Issue 21, pp. 1805-1807, 2008.

[22] S. S. A. Obayya, S. Haxha, B. M. A. Rahman, C. Themistos, and K. T. V. Grattan, "Optimization of the Optical Properties of a Deeply Etched Semiconductor Electrooptic Modulator," *Journal of Lightwave Technology*, vol. 21, No. 8, 2003.

[23] S. Oikawa, F. Yamamoto, J. Ichikawa, S. Kurimura, and K. Kitamura, "Zero-Chirp Broadband Z-Cut Ti: $LiNbO_3$ Optical Modulator Using Polarization Reversal and Branch Electrode," *Journal of Lightwave Technology*, vol. 23, No. 9, 2005.

[24] T. G. Nguyen, A. Mitchell, and Y. S. Visagathilagar, "Investigation of Resonantly Enhanced Modulators on $LiNbO_3$ Using FEM and Numerical Optimization Technique," *Journal of Lightwave Technology*, vol. 22, no. 2, pp. 526-533, 2004.